



Publication Year	2021
Acceptance in OA	2025-02-24T10:09:55Z
Title	The Galactic center chimneys: The base of the multiphase outflow of the Milky Way
Authors	PONTI, Gabriele, Morris, M. R., Churazov, E., Heywood, I., Fender, R. P.
Publisher's version (DOI)	10.1051/0004-6361/202039636
Handle	http://hdl.handle.net/20.500.12386/36149
Journal	ASTRONOMY & ASTROPHYSICS
Volume	646

The Galactic center chimneys: The base of the multiphase outflow of the Milky Way

G. Ponti^{1,2}, M. R. Morris³, E. Churazov^{4,5}, I. Heywood^{6,7,8}, and R. P. Fender⁶

¹ INAF-Osservatorio Astronomico di Brera, Via E. Bianchi 46, I-23807 Merate (LC), Italy
e-mail: gabriele.ponti@inaf.it

² Max-Planck-Institut für Extraterrestrische Physik, Giessenbachstrasse, D-85748, Garching, Germany

³ Department of Physics and Astronomy, University of California, Los Angeles, CA 90095-1547, USA

⁴ Max-Planck-Institut für Astrophysik, Karl-Schwarzschild-Str. 1, D-85748, Garching, Germany

⁵ Space Research Institute (IKI), Profsoyuznaya 84/32, Moscow 117997, Russia

⁶ Astrophysics, Department of Physics, University of Oxford, Keble Road, Oxford OX1 3RH, UK

⁷ Department of Physics and Electronics, Rhodes University, PO Box 94, Makhanda, 6140, South Africa

⁸ South African Radio Astronomy Observatory, 2 Fir Street, Black River Park, Observatory, Cape Town, 7925, South Africa

Received October 9, 2020; accepted December 25, 2020

ABSTRACT

Context. Outflows and feedback are key ingredients of galaxy evolution. Evidence for an outflow arising from the Galactic center (GC) – the so-called GC chimneys – has recently been discovered at radio, infrared, and X-ray bands.

Aims. We undertake a detailed examination of the spatial relationships between the emission in the different bands in order to place constraints on the nature and history of the chimneys and to better understand their impact on the GC environment and their relation with Galactic scale outflows.

Methods. We compare X-ray, radio, and infrared maps of the central few square degrees.

Results. The X-ray, radio, and infrared emissions are deeply interconnected, affecting one another and forming coherent features on scales of hundreds of parsecs, therefore indicating a common physical link associated with the GC outflow. We debate the location of the northern chimney and suggest that it might be located on the front side of the GC because of a significant tilt of the chimneys toward us. We report the presence of strong shocks at the interface between the chimneys and the interstellar medium (ISM), which are traced by radio and warm dust emission. We observe entrained molecular gas outflowing within the chimneys, revealing the multiphase nature of the outflow. In particular, the molecular outflow produces a long, strong, and structured shock along the northwestern wall of the chimney. Because of the different dynamical times of the various components of the outflow, the chimneys appear to be shaped by directed large-scale winds launched at different epochs.

The data support the idea that the chimneys are embedded in an (often dominant) vertical magnetic field, which likely diverges with increasing latitude. We observe that the thermal pressure associated with the hot plasma appears to be smaller than the ram pressure of the molecular outflow and the magnetic pressure. This leaves open the possibility that either the main driver of the outflow is more powerful than the observed hot plasma, or the chimneys represent a "relic" of past and more powerful activity.

Conclusions. These multiwavelength observations corroborate the idea that the chimneys represent the channel connecting the quasi-continuous, but intermittent, activity at the GC with the base of the *Fermi* bubbles. In particular, the prominent edges and shocks observed in the radio and mid-infrared bands testify to the most powerful, more recent outflows from the central parsecs of the Milky Way.

1. Introduction

Outflows and feedback are vital ingredients for the forming and growing of galaxies as we observe them today. Outflows are required in order to connect the activity in the cores and disks of galaxies with the hot, slowly recondensing plasma in their haloes, thereby fostering the evolution of galaxy morphologies (White et al. 1978; 1991; Putman et al. 2012; Tumlinson et al. 2017). Such feedback links the growth of the central supermassive black holes with their coevolving galaxy (Ferrarese & Merritt 2000; Gebhardt et al. 2000; Kauffmann et al. 2003).

As a prototype for typical spiral galaxies, the Milky Way offers a unique opportunity to capture the important details of such feedback all the way from sub-parsec to galactic scales. Indeed, as the Milky Way is located at a distance of only 8.25 kpc (Gravity Col 2020; see also Do et al. 2019, who suggested ~ 7.97 kpc), we can investigate its physical processes at a resolution orders of magnitudes better than in other quiescent galaxies. The most pressing outstanding question is how some portion of the multi-

phase interstellar medium (ISM) can be launched from galactic centers and disks into outflows that replenish galactic coronae, haloes, or even the intergalactic medium with plasma, energy, metals, etc. (Naab et al. 2017). This involves understanding the complex physics of galaxies and their multiphase gas.

The detection of hints of an outflow from the Galactic center (GC) dates back to the 1980s, when sensitive radio maps revealed features with an extent of a few degrees (such as the so-called expanding molecular ring and the Galactic center lobe; GCL), which were originally attributed to large energy releases from the core of the Milky Way (Kaifu et al. 1972; Scoville 1972; Sofue 1984; 1985; 1989). Subsequently, the combination of X-ray (*ROSAT*) and mid-infrared (*IRAS* and *MSX*) observations strengthened this hypothesis, revealing a limb-brightened bipolar structure, possibly the outcome of a large-scale bipolar wind from the GC (Bland-Hawthorn & Cohen 2003). This scenario was then brought to the fore by the discovery of the so-called *Fermi* bubbles, clearly visible above ~ 2 GeV in the *Fermi*

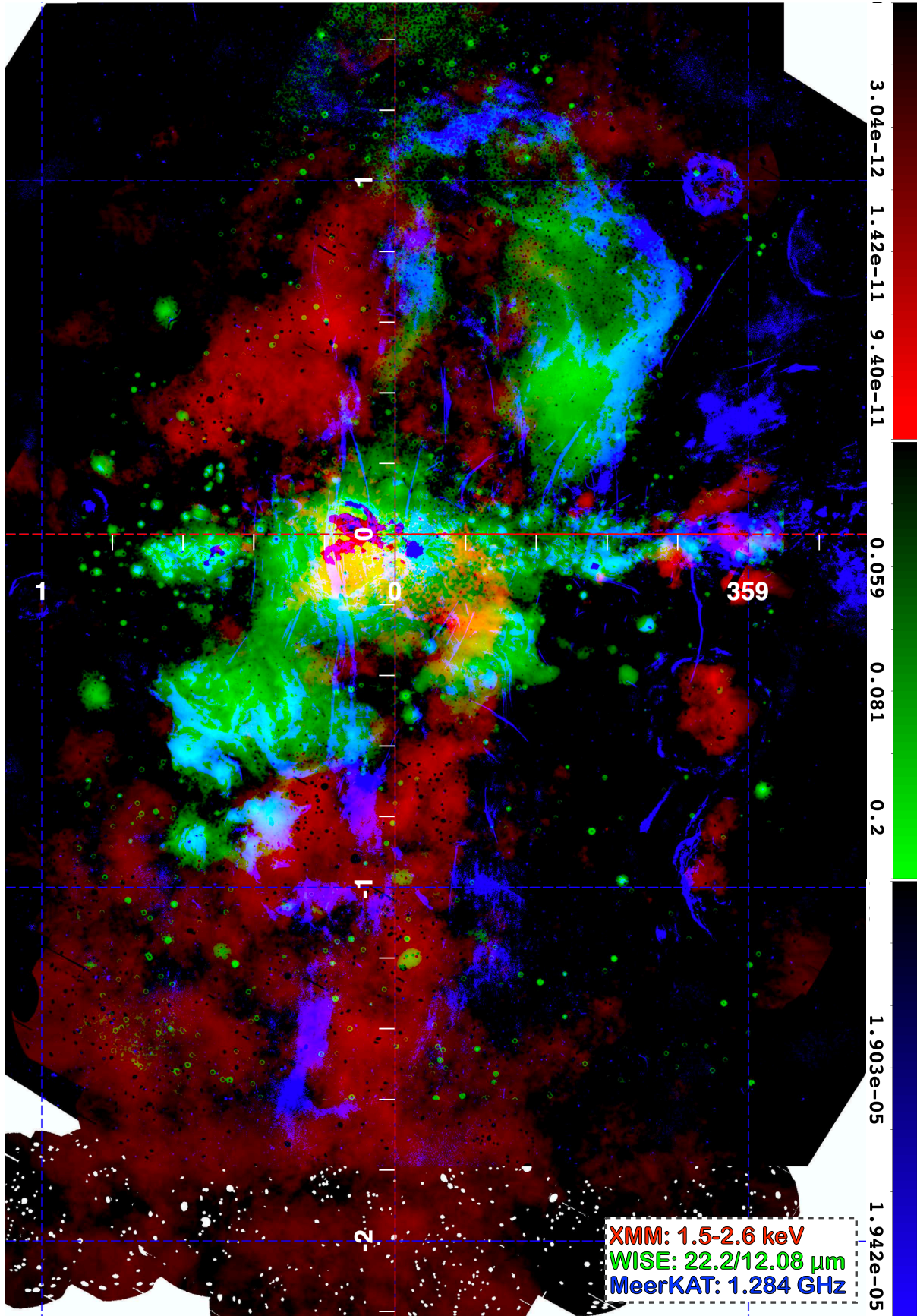


Fig. 1. Multi-phase nature of the GC chimneys. Red, green, and blue show the *XMM-Newton* 1.5-2.6 keV, *WISE* (ratio of 22.2 μm /12.08 μm emission), and *MeerKAT* 1.284 GHz maps, respectively.

data, with a size comparable to the Milky Way itself and a total energy content of $\sim 10^{55}$ erg (Su et al. 2010; Ackermann et al. 2014; Kataoka et al. 2018). It was also suggested that the bases of the *Fermi* bubbles are associated with soft X-ray emission (Bland-Hawthorn & Cohen 2003; Su et al. 2010; Nakashima et al. 2013; Crocker et al. 2015).

Recently, we reported sensitive X-ray maps of the GC, which led us to the discovery of two oppositely directed, 200-pc chimneys of hot plasma connecting the central parsecs with the base of the *Fermi* bubbles (Ponti et al. 2015; 2019; Nakashima et al. 2019). Such chimneys are the smoking-gun evidence of an outflow from the GC (Ponti et al. 2019). Subsequently, radio maps revealed extended radio continuum emission defining two edge-brightened lobes or bubbles, roughly tracing the edges of the X-ray chimneys (Heywood et al. 2019).

Here we examine the X-ray maps jointly with the radio and infrared maps. In Sect. 2, we describe the overlay of the X-ray maps with the radio and infrared ones. In Sect. 3, we discuss the results and then consolidate the observed complexity. Finally, Sect. 4 proposes an emerging simplified picture and details our conclusions.

2. Multiwavelength view of the multiphase GC outflow

The interplay between the various phases of the GC outflow is shown in Figure 1. The red, green, and blue colors show the X-ray (*XMM-Newton*), infrared color ratio ($22.2 \mu\text{m}/12.08 \mu\text{m}$ from *WISE*), and radio (*MeerKAT*) maps, respectively. In red, the continuum-subtracted 1.5-2.6 keV map is shown in logarithmic scale (see Extended Data Fig. 3 of Ponti et al. 2019). Because the X-ray chimneys are primarily thermally emitting, they shine brightly in soft X-ray emission lines. The green shows the ratio of infrared color defined as the $22.2 \mu\text{m}$ *WISE* map divided by the $12.8 \mu\text{m}$ one (see § 2.3 for more details). In blue, the *MeerKAT* map is shown at intensities at or above 2×10^{-5} Jy (see Fig. 1 of Heywood et al. 2019 and note the caveats regarding photometric accuracy in the Methods section). This outstanding color image shows the interplay of the different phases of the GC outflow.

We also note that the *MeerKAT* and *WISE* maps show bright radio and infrared emission associated with G0.5-0.5 and G0.5-0.85, two well-known foreground star formation complexes. Figure 2 shows a finding chart of the region within and just outside of the chimneys, displaying most of the features discussed here.

2.1. Overlay of radio and X-ray maps

Figure 3 shows an X-ray (*XMM-Newton*) and radio (*MeerKAT*) overlay. The thick dashed white line indicates the location of the prominent western edge of the distribution of X-ray emitting plasma defining the chimneys. This appears as a remarkably linear feature with an extent of ~ 350 pc. The thin dashed white line aims at indicating a possible location of the eastern edge of the chimneys; however, its position is less well determined.

We note that both the northern and southern chimneys are prominent in both the X-ray and radio bands, with a striking degree of symmetry with respect to the Galactic plane. However, some asymmetries are clearly evident (Fig. 3).

Toward the northern latitudes, the X-ray emission associated with the GC outflow appears consistent with being edge-brightened (i.e., lacking a ridge of emission at the center of the chimney), although not as much as the radio emission (e.g., see Additional Data Figure 7 of Ponti et al. 2019). This might indi-

cate that the X-ray emission is also produced primarily at the boundaries of the GC outflow, possibly in a structured shock with the ISM. On the contrary, the X-ray emission toward the southern hemisphere peaks along the axis of the chimney, as would be expected if the X-ray emitting plasma is volume filling.

Figure 4 shows the full dynamic range of the *MeerKAT* map, which displays a large array of nonthermal filaments and diffuse radio emission. Some of these filaments are reported in Fig. 2 as dashed gray lines.

2.2. Maps of X-rays versus dense, neutral material

The left panel of Fig. 5 shows in red the soft X-ray emission map (1.5-2.6 keV), in green the S xv line emission (2.35-2.56 keV), and in blue the *MeerKAT* map. The S xv line emission shows clear gradients in rough coincidence with the edges of the *MeerKAT* bubbles. Because of the relatively high brightness and high energy emission of the S xv transition, this emission line provides us with an excellent tool to trace the hot plasma all the way to the Galactic plane. Indeed, it is significantly less affected by interstellar absorption than the soft X-ray emission map. The right panel of Fig. 5 shows the total and continuum-subtracted maps in the 1.5-2.6 keV band in red and blue, respectively. The continuum subtraction efficiently removes the emission from dust scattering haloes around bright sources (e.g., at: (l,b) = (359.98°, 1.26°); (359.56, -0.39); (359.30, -0.88); (359.08, -1.51); (359.12, -0.10); (0.67, 1.18); etc.) as well as nonthermal X-ray sources (e.g., pulsar wind nebulae), as is evident by comparing the red and blue maps. The green color shows the atomic hydrogen column density map of molecular material in a logarithmic scale from 1.2 to $60 \times 10^{23} \text{ cm}^{-2}$ as observed by *Herschel* (Molinari et al. 2011). The highest concentration of molecular material occurs within a few tens of parsecs from the Galactic plane. The high column density of cold material is likely to significantly obscure the X-ray radiation toward the densest regions in the plane (i.e., the Sgr B complex).

A clear depression is observed in the X-ray emission at $b \sim \pm(0.2 - 0.3^\circ)$. We note that foreground absorbing clouds with column densities on the order of $N_H \sim 0.4 - 1 \times 10^{23} \text{ cm}^{-2}$ are present at those locations (Molinari et al. 2011), which is sufficient to account for the observed depressions in X-ray emissivities in terms of increased X-ray absorption.

2.3. The infrared (*WISE*) maps

The *WISE* data were downloaded from the Infrared Science Archive¹ and subsequently mosaicked, adjusting the background to match in the overlapping regions² to obtain a full coverage of the chimneys. The top panels of Fig. 6 show the emission at 12.08 and $22.2 \mu\text{m}$ as observed by *WISE*. As for the dense, neutral material, the highest concentration of warm dust is distributed along the Galactic plane, however showing a considerably larger latitudinal extent. Indeed, spurs of warm dust (the most prominent of which are highlighted by white dashed lines)

¹ <https://irsa.ipac.caltech.edu/applications/wise/>

² We stress that the constant background of each sky tile was adjusted arbitrarily to match in the overlapping regions and to facilitate the display of the various features. In particular, because of the arbitrary subtraction of constant backgrounds and because of the unknown contribution from extended foreground and background emission sources, the map made of the ratio of bands W4 ($22.2 \mu\text{m}$) to W3 ($12.08 \mu\text{m}$) is meant only to be indicative of the trends of dust temperature, and does not provide a quantitative measure of colour temperature.

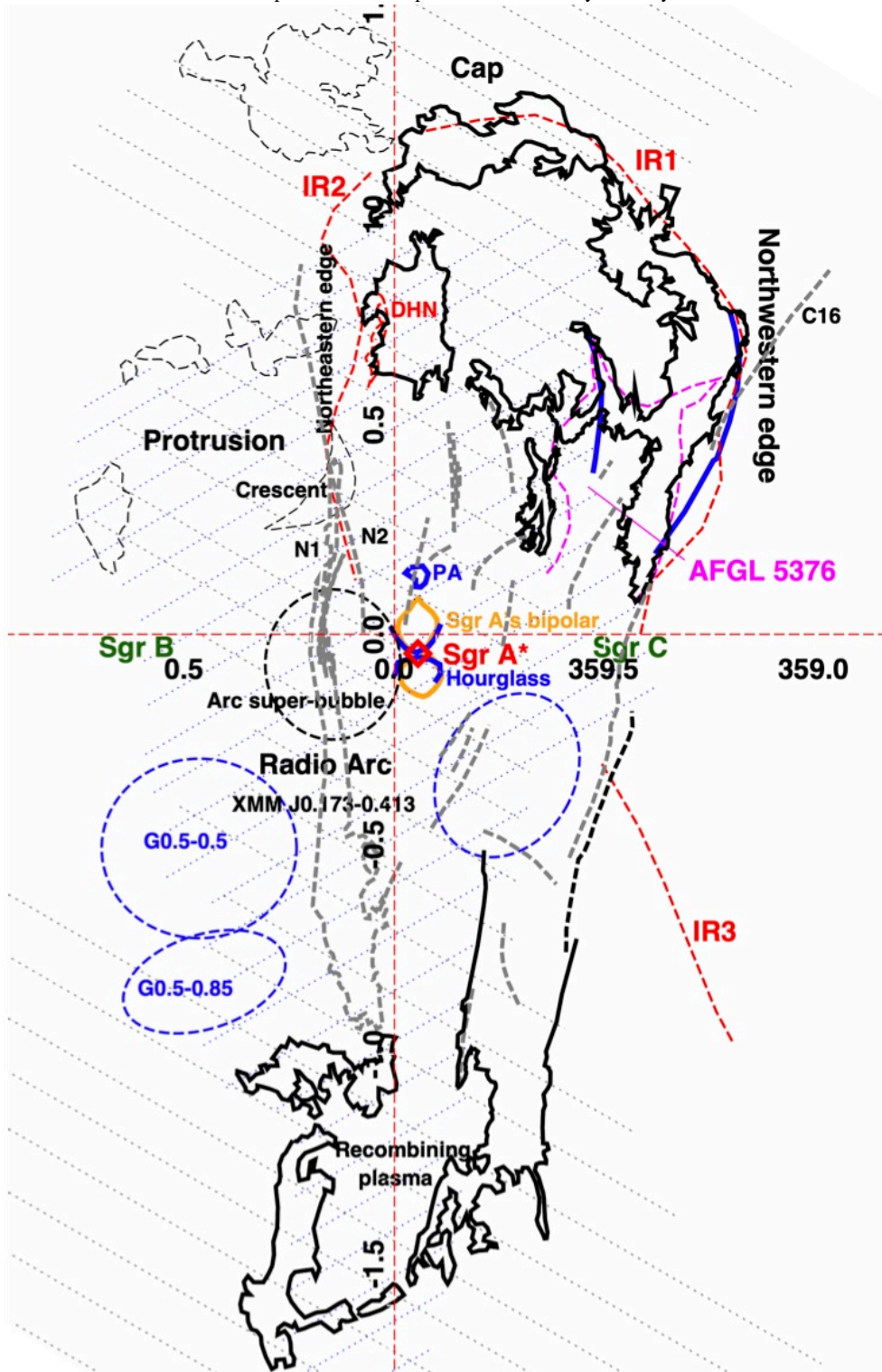


Fig. 2. Finding chart of the region within and just outside the chimneys. The thick-black solid regions show the most prominent radio emitting features clearly associated with the chimneys. The thick dashed gray lines display the locations of the most prominent nonthermal radio filaments (such as N1, N2, XMMJ 0.173-0.413, C16) and of the Radio Arc. The thick-red dashed lines display the location of the spurs of warm dust as evinced from the *WISE* maps and the double helix nebula (DHN; Bland-Hawthorn & Cohen 2003; Enokiya et al. 2014). The magenta dashed lines indicate the borders of the AFGL 5376 feature, as derived from the *WISE* 22.2 μm map (the solid blue lines at this location show the position of the two shocks derived by Uchida et al. 1994). The slanting thin-dotted blue and gray lines show the X-ray emitting region displaying bright S xv and soft X-ray line radiation, respectively. At high latitudes, this emission extends beyond the borders of the chimneys. The thin-black dashed regions show the location of faint radio features appearing at the edges of the X-ray protrusion (§3.6). At the center, a red diamond shows the location of Sgr A*, the orange solid region displays the location of Sgr A's bipolar lobes, as derived from the *XMM-Newton* map, while the blue solid regions show the location of the polar arc (PA) and of the hourglass feature (Hsieh et al. 2016). The latter runs almost perfectly on top of the lower edges of Sgr A's bipolar lobes. The thick-black dashed ellipse shows the location of the Arc super-bubble as it appears in the radio and mid infrared bands, while the thick-blue dashed ellipses show the location of the three well-known foreground star forming regions. The dark green labels indicate the position of the main molecular complexes (the Sgr A complex approximately coincides with Sgr A*).